Remote Sensing of Environment 222 (2019) 65–77

Contents lists available at ScienceDirect

Remote Sensing of Environment

journal homepage: www.elsevier.com/locate/rse

Impact of time on interpretations of forest fragmentation: Three-decades of fragmentation dynamics over Canada

Txomin Hermosilla[a,*], Michael A. Wulder[a], Joanne C. White[a], Nicholas C. Coops[b], Paul D. Pickell[c], Douglas K. Bolton[d]

[a] Canadian Forest Service (Pacific Forestry Centre), Natural Resources Canada, 506 West Burnside Road, Victoria, BC V8Z 1M5, Canada
[b] Integrated Remote Sensing Studio, Department of Forest Resources Management, University of British Columbia, 2424 Main Mall, Vancouver, BC V6T 1Z4, Canada
[c] Department of Forest and Conservation Sciences, University of British Columbia, 2424 Main Mall, Vancouver, BC V6T 1Z4, Canada
[d] Department of Earth & Environment, Boston University, 685 Commonwealth Ave, Boston, MA, USA

ARTICLE INFO

Keywords:
Fragmentation
Disturbances
Temporal analysis
Landsat
Forest
Forest recovery

ABSTRACT

Measures of forest fragmentation, and how fragmentation is changing through time, offer required information for understanding the status and dynamics of forest ecosystems, habitat conditions, and ecosystem functions. In this research, we investigate the multi-temporal characterization of forest fragmentation across the forested ecosystems of Canada (> 650 million ha) and characterize the past three decades of forest fragmentation, providing useful context against which future analyses can be compared. Using 33 years of annual land cover maps produced from classified Landsat image best-available pixel composites (1984–2016), we describe and quantify the different forest patterns and dynamics that emerged in areas that were not disturbed in the analysis period, as well as following stand-replacing (i.e., wildfire, harvest) and non-stand-replacing (e.g., insects, water stress) disturbances. Baseline levels of fragmentation for each ecozone were determined by analyzing unchanged areas. Fragmentation dynamics by dominant forest disturbance showed that harvest activities generally lead to an increase in fragmentation related to the amount of forest cover (composition), while wildfires result in increasing fragmentation as a function of the spatial arrangement of the forest. The results presented herein also allow for characterization of the recovery of vegetation spatial patterns following various disturbance types, with areas dominated by fire presenting slower spatial recovery rates compared to harvest. By the end of the analysis period following disturbance events, forest fragmentation metrics in harvest-dominated landscapes were comparable to the pre-harvesting baseline, reaching 96% of mean pre-disturbance levels for mean forest patch size, and 83% for number of forest patches. In contrast, fire-dominated landscapes resulted in more event related fragmentation, with reduced forest cover (mean Thiel Sen slope = $-0.13\%\ year^{-1}$), mean forest patch size ($-0.22\ ha\ year^{-1}$), an increase in forest patches ($0.11\ year^{-1}$), and forest–non-forest join counts ($0.83\ year^{-1}$). By the end of the analysis period following disturbance events, mean forest patch size reached 52% of mean pre-disturbance levels and 68% the number of forest patches. Overall, non-stand replacing changes had no impact on the behaviour of the forest fragmentation metrics. The open access to Landsat's image archive combined with the analysis methods presented herein enable the systematic quantification and characterization of Canada-wide trends in forest fragmentation trends and post-disturbance spatial patterns over three decades. The results reported herein provide detailed information on the temporal evolution of spatial forest patterns, and illustrate that given an adequate time period, spatial patterns in areas where land use has not changed, recover to resemble pre-disturbance conditions.

1. Introduction

Forest fragmentation refers to the amount and spatial configuration of treed-vegetation (Gustafson, 1998; Riitters et al., 2002) and is driven by both natural (e.g., fires, insects) and anthropogenic (e.g., harvest) processes (Soverel et al., 2010). Forest fragmentation can be related as a state (capture of status) or as a process (relating of change in conditions over time). Increased forest fragmentation results from dissecting contiguous forested areas into smaller and more isolated patches of diverse sizes and shapes (Saunders et al., 1991; Vogelmann, 1995). Changes in

* Corresponding author.
E-mail address: txomin.hermosilla@canada.ca (T. Hermosilla).

https://doi.org/10.1016/j.rse.2018.12.027
Received 12 September 2018; Received in revised form 18 December 2018; Accepted 19 December 2018
Available online 27 December 2018

forest fragmentation have been shown to impact habitat quality, biodiversity patterns and richness, and may ultimately modify the overall ecosystem function and condition of the forest (Fahrig, 2003; Wickham et al., 2008). Forest fragmentation is a dynamic, multidirectional process; fragmentation can vary over time as disturbance and recovery processes interact to alter the amount and spatial configuration of treed-vegetation on a landscape (Pickell et al., 2016a). Thus, monitoring forest fragmentation both spatially and over time is critical for understanding and sustaining a wide variety of ecosystem values (Turner et al., 2013).

Landscape fragmentation can be quantified through a suite of spatial pattern metrics that inform on the amount and configuration of patches, distribution of patch sizes, and edge effects (Betts, 2000). These metrics enable comparison of landscape patterns at different locations, as well as making relative assessments of fragmentation change through time (McGarigal and Marks, 1995; Turner et al., 1989). For large area mapping, it is common to summarize these fragmentation metrics across a regular lattice that partitions a larger area into smaller, regularly-sized landscape units (Cardille et al., 2005; Pickell et al., 2016a; Wulder et al., 2008a).

Historically, due to limited data options (e.g., satellite imagery and related derivations of land cover), fragmentation characteristics over the forested ecosystems were often characterized at a single point in time (Riitters et al., 2000) or by highlighting differences between fragmentation states at epochal time steps, for example bi-temporal (Zheng et al., 1997), 5-yearly (Sanchez-Azofeifa et al., 2001), decadal (Vogelmann, 1995), or longer (Boentje and Blinnikov, 2007). As a process, forest fragmentation, however, is not necessarily well characterized with bi-temporal observations that focus primarily on changes due to forest loss, with limited capacity to capture the return of forests (and concomitant changes in forest pattern) following disturbance. Disturbances operate in a heterogeneous manner and over a range of time scales and play an important role in creating, modifying, and maintaining a spatial mosaic of the vegetation within forested ecosystems (Turner, 1989).

Remotely sensed data enable systematic mapping of forested ecosystems over a range of spatial scales, including regional and global (e.g., Hansen et al., 2013; Hermosilla et al., 2016; Roy et al., 2010). The Landsat satellite program provides decades of high-quality, analysis-ready imagery, at temporal and spatial resolutions suitable for monitoring and mapping natural processes and human activity (Wulder et al., 2008c). As such, Landsat imagery has a key role to play in documenting forest fragmentation patterns and processes (Cohen and Goward, 2004; Vogelmann, 1995). While detailed forest fragmentation analyses covering large areas were traditionally limited to one (Butler et al., 2004; Wulder et al., 2008a) or two observation dates (Wickham et al., 2008), more in-depth, multi-temporal analyses of forest fragmentation were generally spatially constrained (Coops et al., 2010; Li et al., 2009; Pickell et al., 2016a). Continuously monitoring large geographic areas, over multiple decades, at finer time steps, is now a reality following the opening of the United States Geological Survey (USGS) Landsat archive (Woodcock et al., 2008; Wulder et al., 2012). Thus, based upon free and open access to the Landsat archive, novel automated methods that use Landsat time series to generate annual land cover products over large areas are emerging (Gómez et al., 2016; Wulder et al., 2018a).

Landscapes present an inherent level of fragmentation as a consequence of the configuration of topographical and geographical elements, including water features (e.g. rivers, lakes), wetlands, or mountains (Wulder et al., 2011). Natural and anthropogenic disturbances alter this inherent fragmentation of ecosystems, and monitoring this requires multi-temporal information. Detailed knowledge on when and where forest changes occur permits the study of the fragmentation patterns produced by different disturbance drivers. The combined analysis of dense time series of forest maps and detailed forest change data allows for the tracking of forest fragmentation following disturbance events, providing useful information on the temporal evolution of spatial forest pattern, and—given an adequate time period—the recovery of vegetation patterns to resemble pre-disturbance conditions. In this study, we present a comprehensive analysis of forest fragmentation over Canada's forest-dominated ecosystems from 1984 to 2016. As source data, we use annual land cover classification maps (Hermosilla et al., 2018) derived from a time series of Landsat image composites and forest change metrics that were generated using the Composite-to-Change or C2C approach (Hermosilla et al., 2016). The objectives of this study were threefold: (i) to quantify and characterize national and regional trends in forest fragmentation (1984–2016); (ii) to capture and map baseline levels of forest fragmentation in forest areas that have not changed over the analysis timeframe; and (iii) to quantify and analyze the different dynamics and changes to forest fragmentation patterns following natural and anthropogenic disturbance events, relative to the baseline levels of fragmentation.

2. Study area

Canada's forested ecosystems comprise ~650 million ha, or 65% of Canada's total area (998.5 million ha) (Wulder et al., 2008b). These forest-dominated ecozones are mainly a mixture of trees, shrubs, wetlands, and lakes, with treed and other wooded lands occupying 347.1 million ha (Natural Resources Canada, 2016). Fires are the main stand-replacing disturbance, impacting an estimated 40.6 million ha between 1985 and 2010, compared to the 16.7 million ha that were harvested over that same 25-year period (White et al., 2017). The forest dominated ecosystems are identified following the ecozone stratification of Canada (Ecological Stratification Working Group, 1995) shown in Fig. 1. As the Boreal Shield and Taiga Shield ecozones have large longitudinal extents and consequently a broad range of ecoclimatic conditions from west to east, these ecozones are partitioned into a western and eastern component (Frazier et al., 2015; Stocks et al., 2002).

3. Methods

3.1. Data

3.1.1. Landsat time series data and derived forest change information

Forest change information was generated using the Composite-2-Change or C2C approach (Hermosilla et al., 2016). The C2C approach comprises the generation of annual best-available pixel (BAP) image composites by choosing optimal observations for each pixel from all available archived Landsat-5 TM, Landsat-7 ETM+, and Landsat-8 OLI imagery with < 70% cloud cover (Hermosilla et al., 2017). Input Landsat images are atmospherically corrected to surface reflectance using LEDAPS (Masek et al., 2006; Schmidt et al., 2013). Optimal observations are chosen based on the scoring functions defined by White et al. (2014) and Hermosilla et al. (2015a), which include proximity to mid-summer target date (Julian day 213 ± 30 days), presence and distance to clouds and their shadows (detected using Fmask algorithm, Zhu and Woodcock, 2012), atmospheric quality, and acquisition sensor (Landsat-7 ETM+ is penalized after scan line corrector failure in 2003). These annual composites are further refined by removing noisy observations (e.g. unscreened clouds and haze) and by infilling data gaps (due to a lack of suitable observations) with proxy values by applying spectral trend analysis to each pixel-level time series (Hermosilla et al., 2015a). Temporal trends and changes are determined with a bottom-up/sliding window (SWAB) breakpoint detection algorithm (Keogh et al., 2001) using Normalized Burn Ratio (NBR) values as inputs (Key and Benson, 2006). The SWAB algorithm divides the pixel series, composed of n segments, into n-1 segments and assesses the cost of merging pairs of adjacent segments (using root mean square error) based on the lowest cost. This process is iterated until the maximum

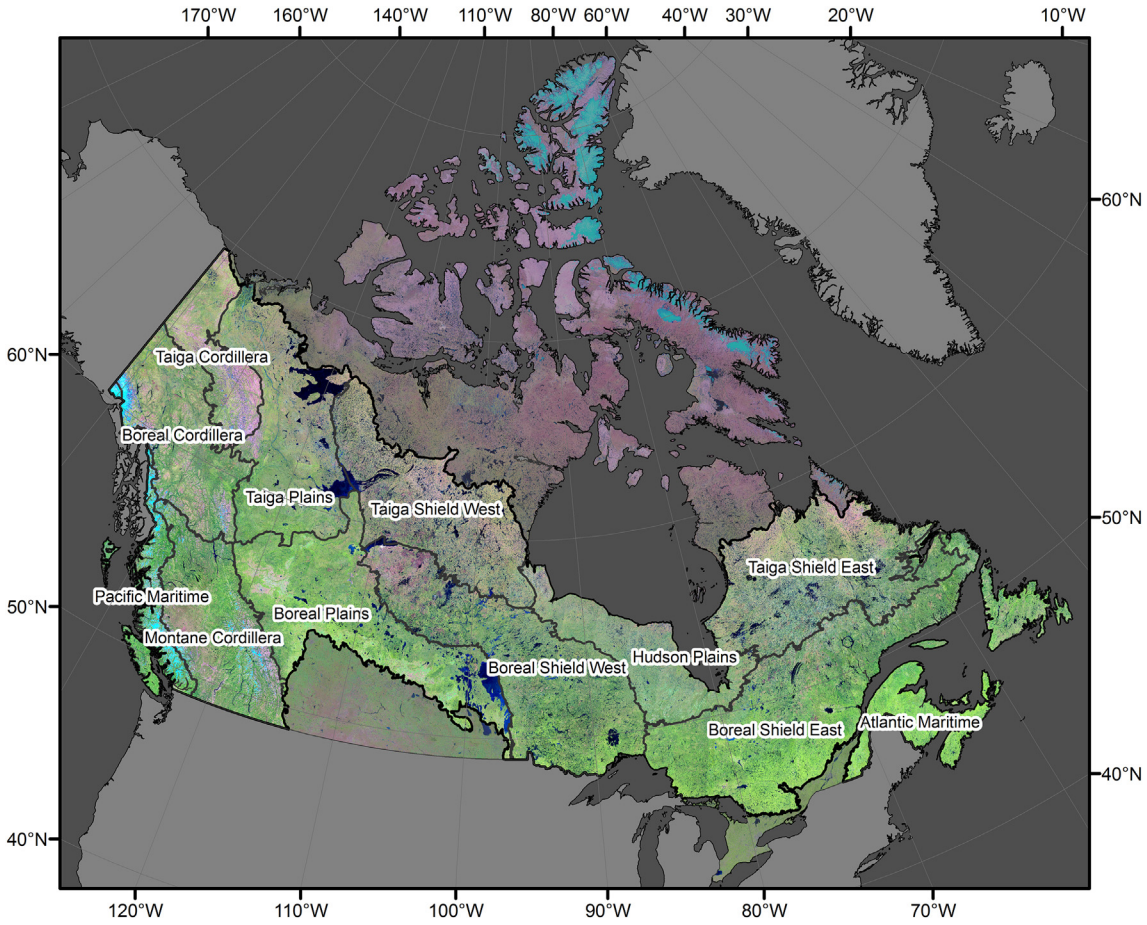

Fig. 1. False-color Landsat best-available-pixel (BAP) composite of Canada in 2010 overlaid with Canada's forested ecozones.

Table 1
Summary of landscape units comprised by the analysis strata.

Stratum	Landscape units
All	5,626,672
Unchanged	3,401,892
Wildfire dominated	722,487
Harvesting dominated	249,995
Non-stand replacing change dominated	244,424

number of segments (six) are used or the maximum allowable merging cost (0.125) is reached (Hermosilla et al., 2017). Following breakpoint detection, segments and trends are identified, that are in turn used to define a set of descriptive metrics that characterize the change events (e.g. magnitude) as well as pre- and post-change conditions. This analysis in the temporal domain is then followed by analysis in the spatial domain, with the objective of improving the spatial homogeneity and consistency of the change detection. At this stage in the processing, change events with an area smaller than the minimum mapping unit (0.5 ha) are removed (Hermosilla et al., 2015a). Utilizing the full temporal depth of Landsat images from over 1280 scenes (path/row) resulted in seamless annual surface reflectance composites for all of Canada from 1984 to 2016, as well as the detection and characterization of forest change events (Hermosilla et al., 2017, 2016). Changes were then attributed to a change type (i.e., fire, harvest) based on their spectral, temporal, and geometrical characteristics, using a Random Forest classifier following the object-based image analysis approach presented in Hermosilla et al. (2015b). Validation using independent data indicated an overall accuracy of 89% on detection of change (change, 92%; no change, 88%) and 92% overall on change attribution with greater accuracy found for the stand replacing disturbances of wildfire and harvest (96%). With regards to timing of change, 89% of changes are assigned to the correct year, with 98% within ± 1 year (Hermosilla et al., 2016). Landsat-derived forest change information is available online and can be freely downloaded from https://opendata.nfis.org/mapserver/nfis-change_eng.html.

3.1.2. Land cover maps

Treed areas were derived from the annual land-cover maps of Canada for 1984 to 2016 generated using the Virtual Land Cover Engine (VLCE) framework described in (Hermosilla et al., 2018). These 30-m spatial resolution maps are derived from the spectral information provided by the Canada-wide pixel composites (Hermosilla et al., 2017, 2016) combined with topographic data using a Random Forests classifier. Then, a Hidden Markov Model was applied to incorporate disturbance information and year-to-year vegetation succession expectations and expert-based class transition likelihoods (Abercrombie and Friedl, 2016; Gómez et al., 2016), which resulted in disturbance informed, temporally integrated, land-cover maps. These maps comprise 12 land-cover classes, including non-vegetated (i.e., water, snow/ice, rock/rubble, exposed/barren land), vegetated non-treed (i.e., bryoids, herbs, wetland, shrubs), and treed-vegetation (i.e., wetland-treed, coniferous, broadleaf, mixedwood) after Wulder et al. (2008b). The reported accuracy on the discrimination between treed-vegetation, vegetated non-treed, and non-vegetated is 82.5%. Refer to Hermosilla et al. (2018) for more information on the land cover products used herein.

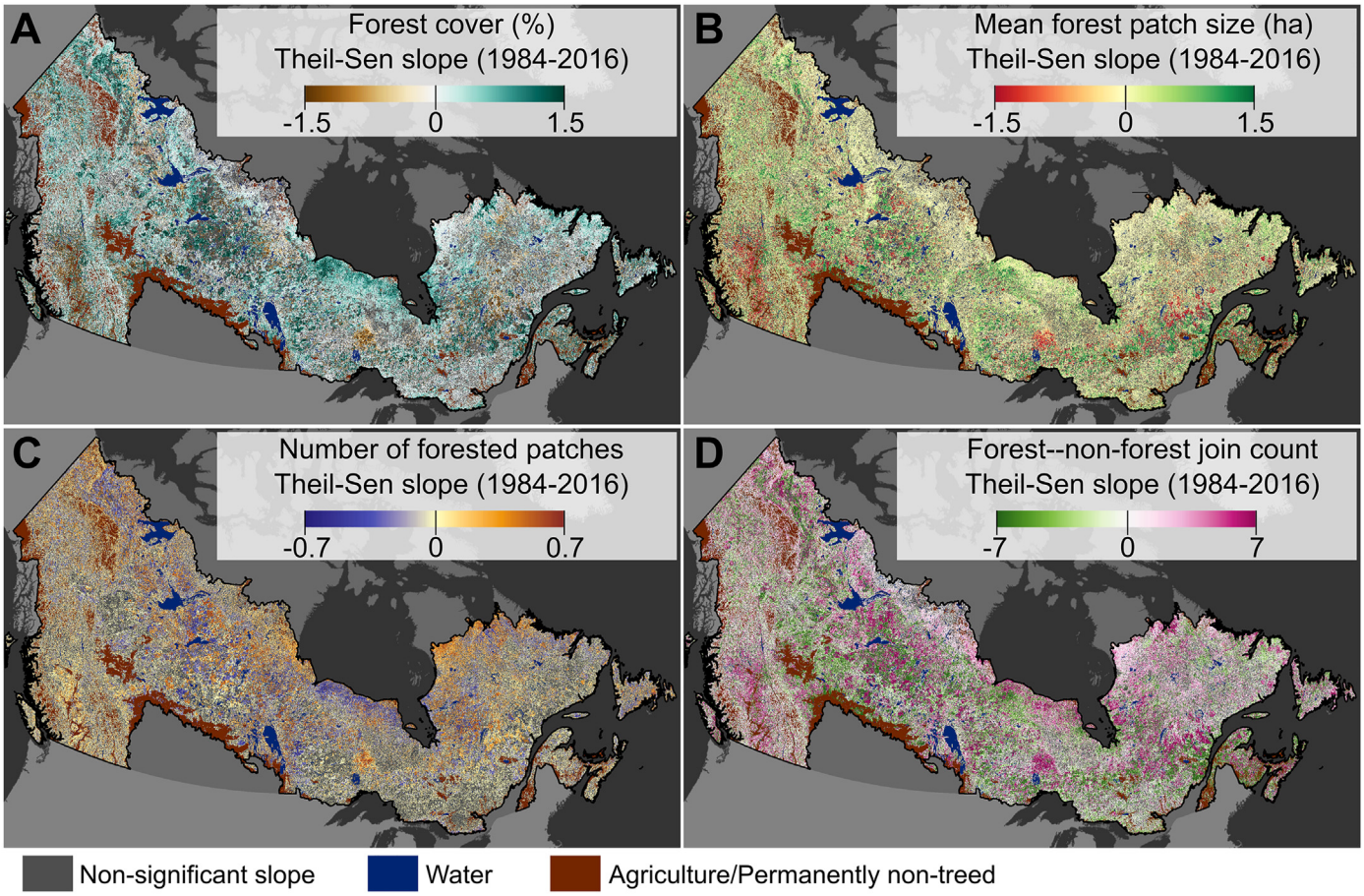

Fig. 2. Theil-Sen slopes for the forest fragmentation metrics (a) forest cover, (b) mean forest patch size, (c) number of forested patches, and (d) forest–non-forest join count, across Canada's forested ecosystems (1984–2016). Only significant slopes are displayed, which was determined using the Mann-Kendall test. Note that values above/below the upper/lower limits are truncated for the purposes of graphical representation. Legends only applicable within Canada's forested ecosystems.

3.2. Forest fragmentation metrics and analysis

Fragmentation metrics were computed on a 1 × 1 km grid of landscape analysis units covering Canada's forested ecosystems (6,505,207 in total). As supported by Wulder et al. (2008a), analysis units of this size allow for sufficient capture and representation of local detail in spatial pattern, while also capturing the patterns imposed by the dominant stand-replacing disturbance agents in Canada: wildfire and harvest. First, the 12-class land cover maps were reclassified into three classes: forest, non-forest, and other, with the forest class containing all treed-vegetation categories. The non-forest class contained the non-treed vegetation categories as well as exposed/barren land, while the "other" class referred to those land cover categories that are considered invariant with regards to forest fragmentation, including water, snow/ice, and rock/rubble (Wulder et al., 2008a). In total, four key fragmentation metrics were computed for each landscape analysis unit (i.e. 1 × 1 km cell) for each year: forest cover, mean forest patch size, number of forested patches, and forest–non-forest join counts. Forest cover is the percentage of a given landscape unit occupied by treed-vegetation. This metric is indicative of forest dominance, with higher values indicating more forest cover relative to non-forest cover classes (Li et al., 2005; Pickell et al., 2016a). Mean forest patch size is the average size in hectares of the portion of treed patches contained within the landscape unit. Smaller mean sizes are indicative of more fragmentation (McGarigal and Marks, 1995). The number of forested patches indicates the number of patches that comprise treed vegetation in a landscape unit. As the area of the landscape units do not vary, a larger number of forested patches indicate a more fragmented forest (McGarigal and Marks, 1995; Turner, 1989). The forest–non-forest join count relates the frequency of forest and non-forest pixel adjacencies or edges, and is indicative of the configuration of treed vegetation (Boots, 2005; Riitters et al., 2002). The forest–non-forest join count metric is lowest for both high and low forest cover and reaches a maximum at 50% forest cover (Long et al., 2010).

Landscape units with notable agricultural (> 3%) or water (> 90%) areas, and without treed vegetation through the analysis period (< 0.5%) were excluded from the analysis, resulting in 5,626,672 landscape units. For analysis purposes, we stratified the landscape units based on the dominant disturbance type, including unchanged (landscape units with < 10% of the area disturbed 1984–2016), fire, harvesting, and non-stand replacing change (Hermosilla et al., 2015b). We stratified landscape units by dominant disturbance type (i.e. wildfire, harvest, or non-stand replacing) when > 35% of the landscape unit area was affected by that disturbance type over the time series. Since a landscape unit may be impacted by multiple changes in different years, each landscape unit and change type was assigned the most frequent year of area changed for the dominant change type (hereafter referred to as the modal year of disturbance). The resulting number of landscape units in each stratum is summarized in Table 1.

Changes in annual fragmentation values were assessed for each metric using Theil-Sen non-parametric regression (Sen, 1968). The Theil-Sen approach calculates all pairwise slopes for a given fragmentation metric through time by landscape unit (1984–2016) and returns the median slope. Theil-Sen slopes are less sensitive to outliers than traditional linear regression and are therefore more commonly used in time series analyses (Pickell et al., 2016a; Rickbeil et al., 2018). Slope

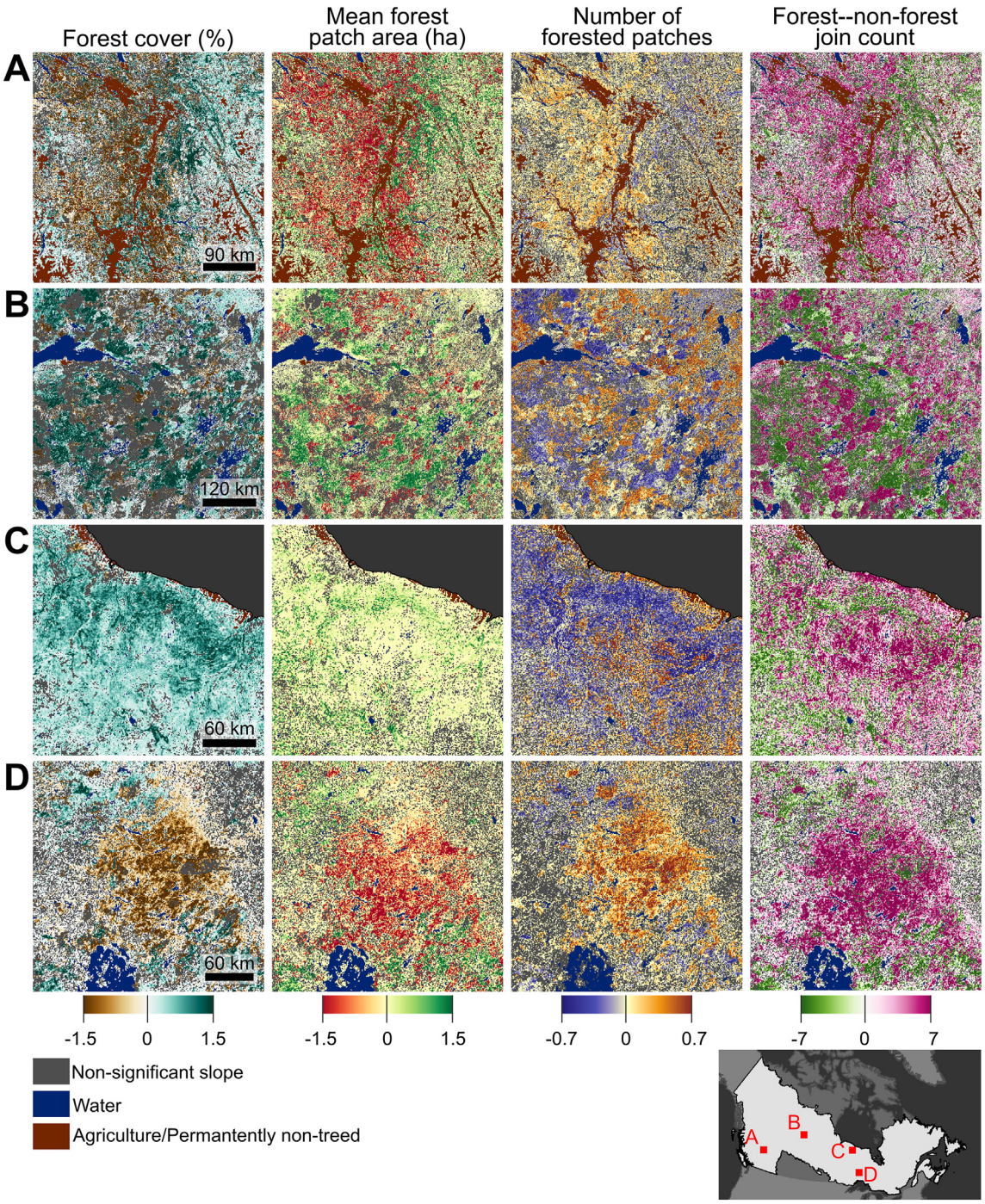

Fig. 3. Details of Theil-Sen slopes for the forest fragmentation metrics (1984–2016) showing (a) Montane Cordillera, (b) boundary between Taiga Shield West and Boreal Shield West, (c) Hudson Plains, and (d) Boreal Shield East. Only significant slopes are displayed, which was determined using the Mann-Kendall test. Note that values above/below the upper/lower limits of the portrayed data ranges are truncated for the purposes of graphical representation. Legends only applicable within Canada's forested ecosystems.

significance was computed using nonparametric Mann–Kendall test (Kendall and Gibbons, 1990). The Mann-Kendall tests for monotonic trends, while the Thiel-Sen estimator provides the sign and magnitude for those trends.

4. Results

The results presented herein focus on three different aspects. First, we provide a national assessment of temporal trends in forest fragmentation metrics across all landscape units, for both disturbed (i.e. wildfire, harvest, non-stand replacing) and undisturbed units. Then, to establish a forest fragmentation baseline for each ecozone, we characterize the fragmentation of the landscape units that were not disturbed during our analysis period (1984–2016). Finally, we present a detailed analysis of the evolution of forest fragmentation dynamics following natural (i.e., fire, non-stand replacing changes) and anthropogenic (i.e., harvesting) disturbance events, and compare those to baseline levels of fragmentation derived from unchanged landscape units.

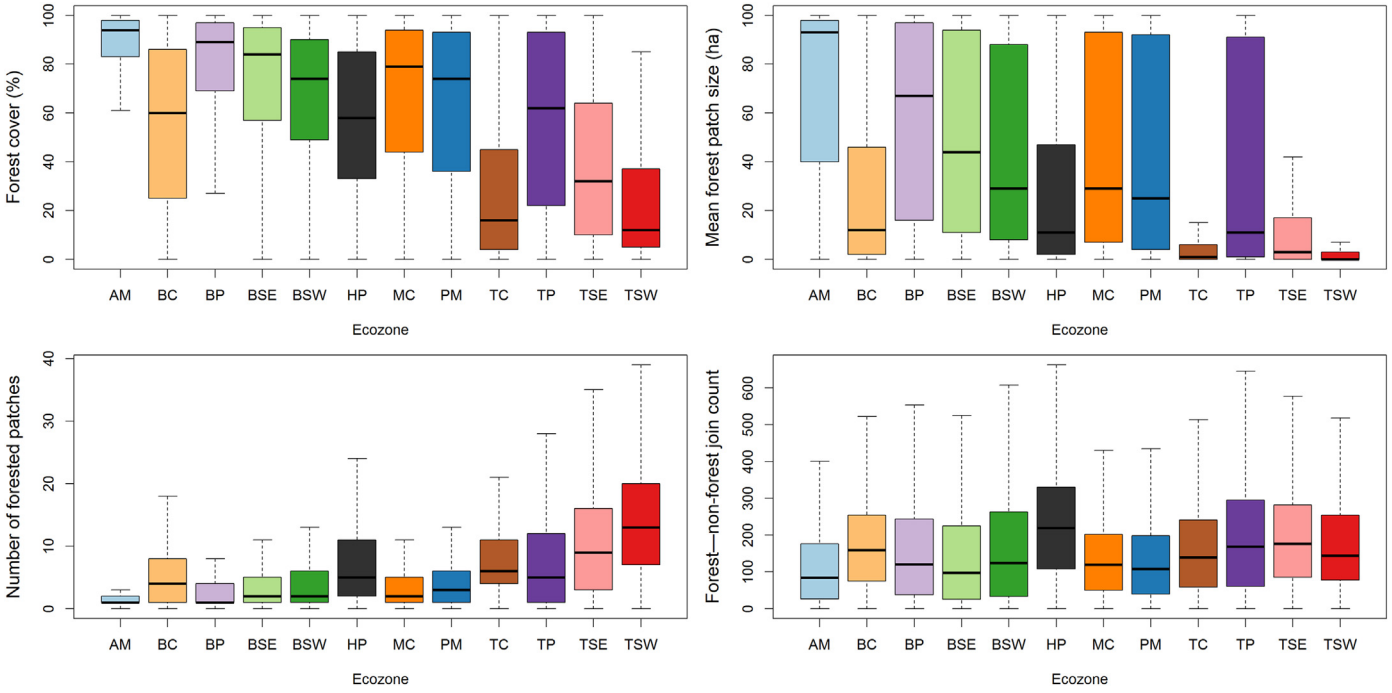

Fig. 4. Distribution of forest fragmentation metrics: (a) forest cover, (b) mean forest patch size, (c) number of forested patches, (d) forest–non-forest join count, in unchanged landscape units by forested ecozone for 1984–2016. (AM: Atlantic Maritime; BC: Boreal Cordillera; BP: Boreal Plains; BSE: Boreal Shield East; BSW: Boreal Shield West; HP: Hudson Plains; MC: Montane Cordillera; PM: Pacific Maritime; TC: Taiga Cordillera; TP: Taiga Plains TSE: Taiga Shield East; TSW: Taiga Shield West). Boxplots represent median, interquartile range, and extreme values. Note that outliers are not displayed.

Table 2
Summary statistics of forest fragmentation metrics by ecozone in unchanged landscape units.

Ecozone	Forest cover [%]			Mean forest patch size [ha]			Number of forested patches			Forest–non-forest join count		
	Mean	Median	St. dev.	Mean	Median	St. dev	Mean	Median	St. dev.	Mean	Median	St. dev.
Atlantic Maritime	83.9	93.0	21.0	66.0	91.0	37.1	2.8	1.0	4.0	131.0	96.0	121.3
Boreal Cordillera	55.2	60.0	32.8	30.1	11.0	36.2	5.6	4.0	5.0	172.8	160.0	116.4
Boreal Plains	77.6	88.0	25.5	55.9	48.0	39.9	4.1	1.0	5.5	157.9	126.0	135.4
Boreal Shield East	71.9	82.0	27.4	50.0	42.0	39.4	4.4	2.0	5.7	142.5	106.0	130.6
Boreal Shield West	66.1	73.0	27.4	41.1	27.0	37.5	5.1	2.0	6.0	163.1	128.0	142.7
Hudson Plains	55.0	55.0	30.0	28.3	9.0	35.9	8.2	5.0	8.1	228.7	222.0	141.3
Montane Cordillera	65.9	77.0	31.4	43.3	28.0	39.3	3.9	2.0	3.8	139.9	124.0	104.7
Pacific Maritime	62.5	72.0	32.6	40.4	23.0	39.3	4.3	3.0	4.2	133.4	115.0	104.1
Taiga Cordillera	27.6	16.0	28.5	9.3	1.0	21.2	7.9	7.0	5.9	161.5	140.0	119.0
Taiga Plains	55.8	60.0	35.3	34.3	10.0	40.6	7.6	5.0	7.8	190.6	172.0	142.3
Taiga Shield East	38.4	32.0	30.5	16.5	2.0	28.3	10.8	9.0	8.8	193.1	180.0	126.2
Taiga Shield West	23.6	12.0	25.1	6.8	0.0	18.0	14.1	13.0	8.7	174.3	144.0	121.0

4.1. Canada's forest fragmentation dynamics 1984–2016

The analysis of Canada's forest fragmentation dynamics was conducted by analyzing the Theil-Sen slopes for the forest fragmentation metrics between 1984 and 2016 for all 1 × 1 km cells, regardless of disturbance history. Maps of the national Theil-Sen slopes computed at landscape unit level (1 × 1 km) are shown in Fig. 2, which displays areas of both increasing and decreasing fragmentation trends (Fig. 3). Areas of increasing fragmentation are generally characterized by decreases in forest cover, decreases in mean forest patch size, and increases in number of forested patches and number of forest–non-forest joins. Alternatively, areas where forest fragmentation was decreasing experienced increasing forest cover and mean forest patch size, as well as a decrease in the number of forested patches. The forest–non-forest join count exhibited variable behaviour depending on the initial forest cover, with positive trends in areas characterized by scant treed-vegetation.

4.2. Baseline forest fragmentation

To establish a forest fragmentation baseline for each ecozone, we computed the 33-year distribution of the values of the fragmentation metrics in unchanged landscape units, by forested ecozone (Fig. 4 and Table 2). The combined analysis of the metrics indicates that the Taiga Shield West, Taiga Shield East, and Taiga Cordillera are the most fragmented ecozones, with the lowest forest cover and mean forest patch size median values, the narrowest interquartile range for mean forest patch size, and the largest number of forested patches. In contrast the Atlantic Maritime, Boreal Plains, and Boreal Shield East are the least inherently fragmented ecozones, with the highest forest cover and mean forest patch size median values, and the lowest number of forested patches. Hudson Plains and Boreal Cordillera have average to high forest cover, but relatively lower forest patch area and greater number of forested patches. Moreover, the Hudson Plains has the highest forest–non-forest join count. The metrics indicate that the Hudson Plains and Boreal Cordillera are composed of abundant treed

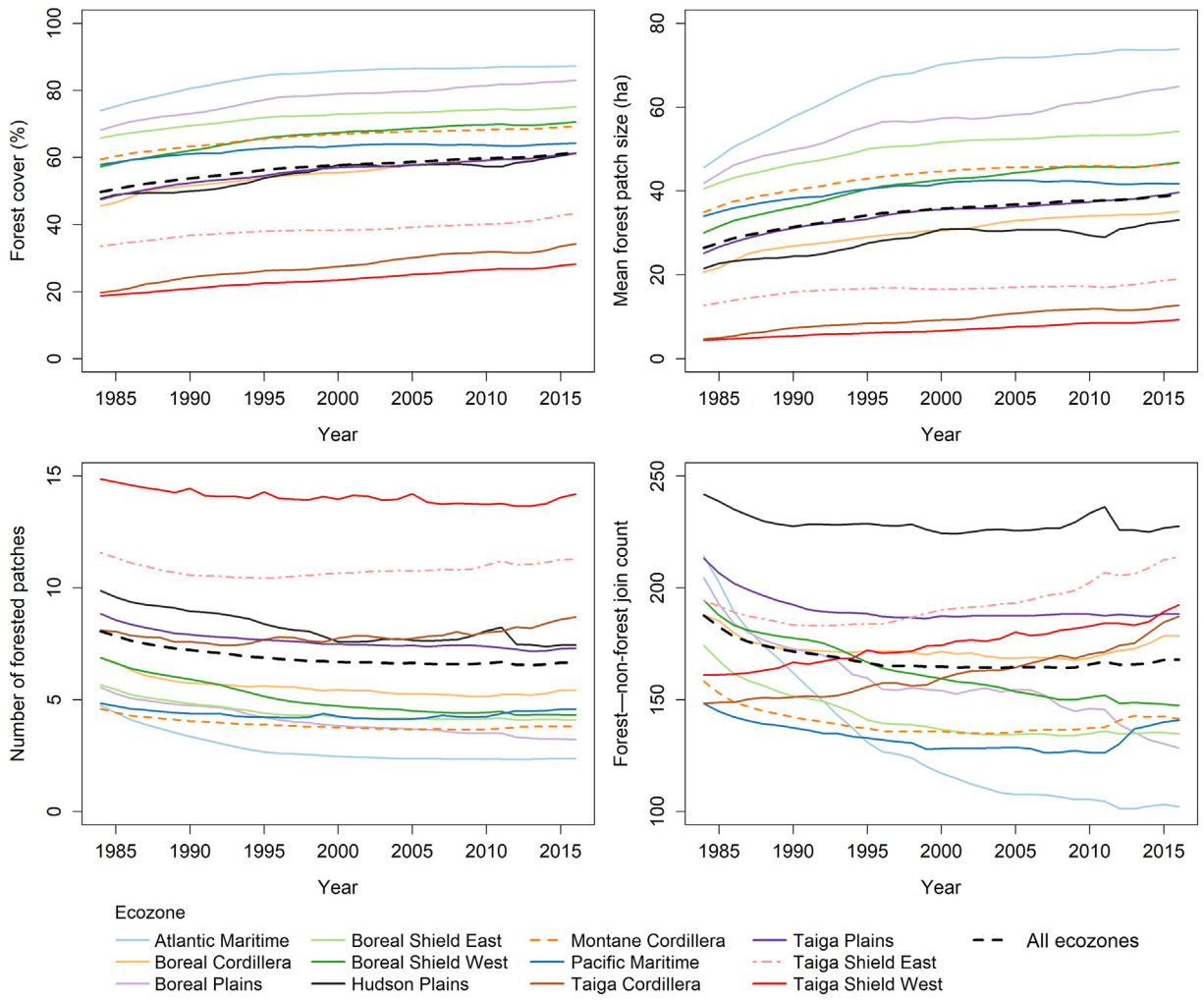

Fig. 5. Mean annual values of forest fragmentation metrics (a) forest cover, (b) mean forest patch size, (c) number of forested patches, and (d) forest –non-forest join count, in unchanged landscape units nationally (all ecozones) and by forested ecozone for 1984–2016.

vegetation, but it is spatially arranged in numerous and small forested patches (such as in among wetlands or in alpine areas).

The mean annual values of the forest fragmentation metrics analyzed for unchanged landscape units (i.e., units that did not undergo disturbances during the analyzed period) across Canada's forested ecosystems is shown in Fig. 5. Over the analysis period (1984–2016) all metrics display significant temporal trends (all p-values < 0.001 for the Mann-Kendall test). Forest cover and mean forest patch area increased over the time period (0.35% and 0.29% mean Thiel-Sen slopes for significant trends, respectively). In contrast, the number of forested patches and forest–non-forest join count decreased over the time period (-0.04 and -0.45 mean Thiel-Sen slopes, respectively). Analyzing the results by ecozone, forest cover and mean forest patch area show positive trends for all ecozones. Forest cover mean Thiel-Sen slopes ranged from 0.19% in Pacific Maritime to 0.46% in Boreal Plains. Mean forest patch size mean Thiel-Sen slopes ranged from 0.11% in Taiga Shield East to 0.61% in Atlantic Maritime. These trends are generally steeper during the first years of the time series analyzed (before 1995), which is most pronounced in ecozones with highest mean forest cover values (i.e., Atlantic Maritime, Boreal Plains, Boreal Shield East). This is likely an artifact of recovering forests that were disturbed prior to the analysis period (i.e., pre-1984; see Section 5.2 for further discussion on disturbance timing relative to analysis period). The mean annual number of forested patches decreased for most ecozones (ranging from -0.095 mean Thiel-Sen slope in Boreal Shield West to -0.002 in Pacific Maritime) with the exception of Taiga Cordillera (0.026) and Taiga Shield East (0.013), however the overall magnitude of the trends in forest patch size was small. Forest–non-forest join count increased for ecozones characterized by low forest cover (i.e., Taiga Shield West [1.03 mean Thiel-Sen slope], Taiga Shield East [0.92], Taiga Cordillera [1.18]), and decreased for ecozones with the highest forest cover values (i.e., Atlantic Maritime [-3.28], Boreal Plains [-1.94], Boreal Shield West [-1.52], and Boreal Shield East [-1.11]).

4.3. Forest fragmentation trends & disturbance events

To analyze the impact of disturbances on forest fragmentation dynamics, we stratified the results by dominant disturbance (i.e., unchanged, fire, harvesting, and non-stand replacing changes). The Canada-wide distribution of Theil-Sen slope values for the forest fragmentation metrics stratified by dominant disturbance for 1984–2016 is shown in Fig. 6. Landscape units with no changes presented positive slopes for both forest cover and mean forest patch size metrics, slightly negative for number of forested patches, and balanced for forest–non-forest join count. Harvest-dominated landscape units displayed the lowest negative Thiel-Sen slopes for mean forest patch size metrics and the largest positive slopes for forest–non-forest join counts. Landscape units dominated by fires exhibited larger positive Thiel-Sen slopes for number of forested patches. Overall, non-stand replacing disturbances resulted in a Thiel-Sen slope distribution similar to the unchanged landscape units. Fig. 7 presents the distribution of the Theil-Sen slope values by ecozone for the forest fragmentation metrics stratified by

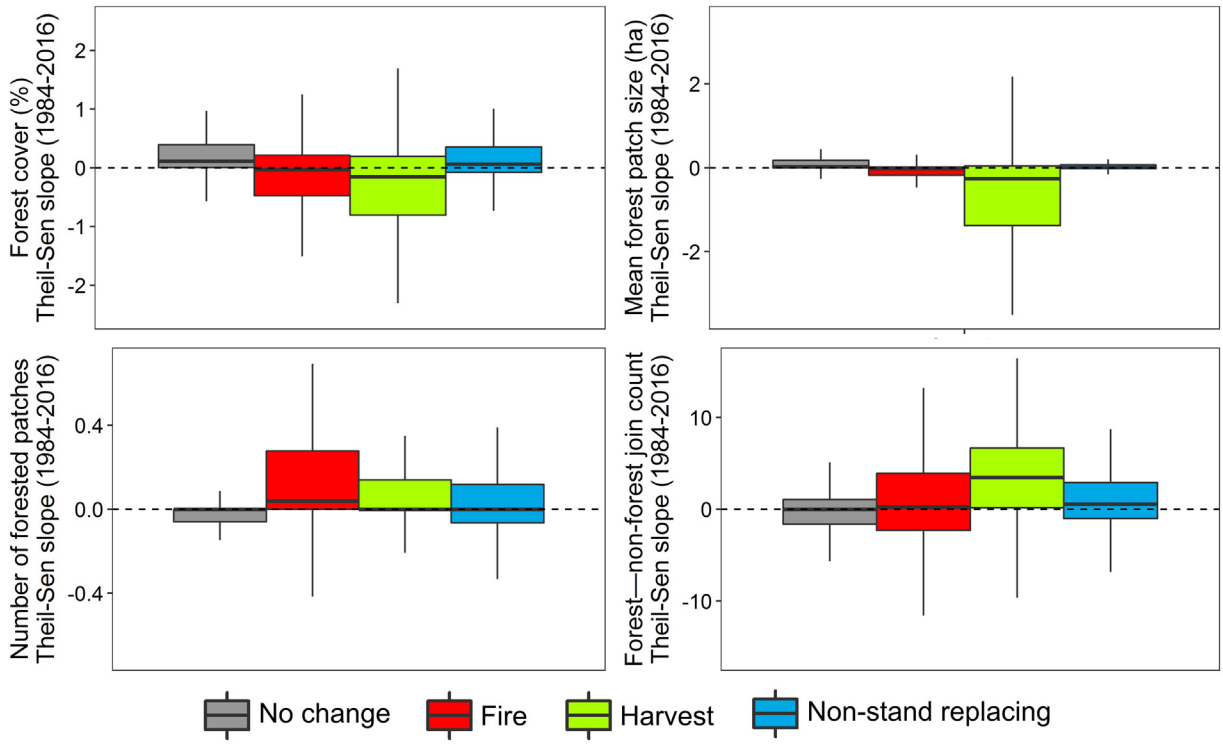

Fig. 6. Distribution of the Theil-Sen slopes of the forest fragmentation metrics (a) forest cover, (b) mean forest patch size, (c) number of forested patches, and (d) forest–non-forest join count, across Canada's forested ecosystems. Boxplots represent median, interquartile range, and extreme values. Note that outliers are not displayed.

dominant disturbance for 1984–2016. Overall, fire-dominated landscape units were associated with a moderate reduction of forest cover and increased number of forest patches. The four metrics analyzed indicate an increase in forest fragmentation (1984–2016) in the Montane Cordillera, Boreal Cordillera, and Boreal Plains. Non-stand replacing changes result in balanced distributions of Theil-Sen slopes with medians close to zero.

To study the development of forest fragmentation and the spatial recovery of treed-vegetation patterns following natural and anthropogenic disturbance events, we monitored the evolution of the forest fragmentation metrics related to time since disturbance. The annual mean values of the forest fragmentation metrics in disturbance-dominated landscape units (i.e., fire, harvesting, and non-stand replacing changes) are shown in Fig. 8. Note that the sample population across the analyzed period is variable, with a greater number of landscape units within a shorter time since the modal disturbance year and a lesser number of landscape units with longer periods of time since disturbance. This distribution produces more unstable trends at the end of the analyzed period (i.e., tail of the time-since-disturbance distribution). Thus, results produced from a smaller number of landscape units is noted and consequently should be more cautiously interpreted. Harvesting events tend to occur in less fragmented landscapes compared with fires: pre-harvest forest cover and mean forest patch size are higher, number of patches is lower, and forest–non-forest join count is lower. Following harvest, forest fragmentation evolves towards the pre-change condition at a higher rate compared with fires. By the end of the 30-year post-change analysis period, forest fragmentation metrics in harvest-dominated landscapes are comparable to the pre-harvesting baseline. The sustained and continued increase in mean forest patch size over time following harvest events is expected to cease when the maximum available area within the landscape unit is reached. In contrast, fire-dominated landscapes resulted in more fragmentation, with a reduction of forest cover and mean forest patch size, and increase of forest patches and forest–non-forest join counts. Overall, non-stand replacing changes have little effect on the behaviour of the forest fragmentation metrics.

Chronosequences showing the relationship between initial forest cover and 0, 10, 20, and 30 years following the modal disturbance year for the disturbance classes are presented in Fig. 9. As expected, harvesting occurs in landscapes with high initial forest cover and after 20 years most harvest-dominated landscapes exhibit high forest cover. Fire-dominated landscapes tend to have lower initial forest cover and take up to 30 years to approximate the pre-fire initial forest cover level indicating slower recovery rates compared with harvests. Non-stand replacing changes have little effect on the level of fragmentation found, with most of the values distributed around the 1:1 diagonal line following the modal disturbance year.

5. Discussion

5.1. Characterization of forest fragmentation dynamics in Canada's forested ecosystems from 1984 to 2016

The results presented herein enable the establishment of a baseline of forest fragmentation, and a capacity to monitor fragmentation dynamics following disturbance across Canada's forested ecosystems. The analysis of the areas that have not been affected by disturbances during the analysis period characterize the forest fragmentation baseline for each forested ecozone that has resulted from the spatial distribution of treed vegetation in relation to the topography and the presence of largely invariant physical features (e.g., lakes), as well as the disturbance history of the unit prior to our time series (i.e. prior to 1984) (Pekel et al., 2016; Wulder et al., 2011). This baseline is useful for comparative purposes and to understand the legacy of disturbance on forest pattern within the various ecozones. Using this baseline, we can determine which ecozones had relatively higher (i.e. Taiga Shield West, Taiga Cordillera) or lower levels of forest fragmentation (i.e., Atlantic Maritime, Boreal Plains). Furthermore, examining the trends in annual

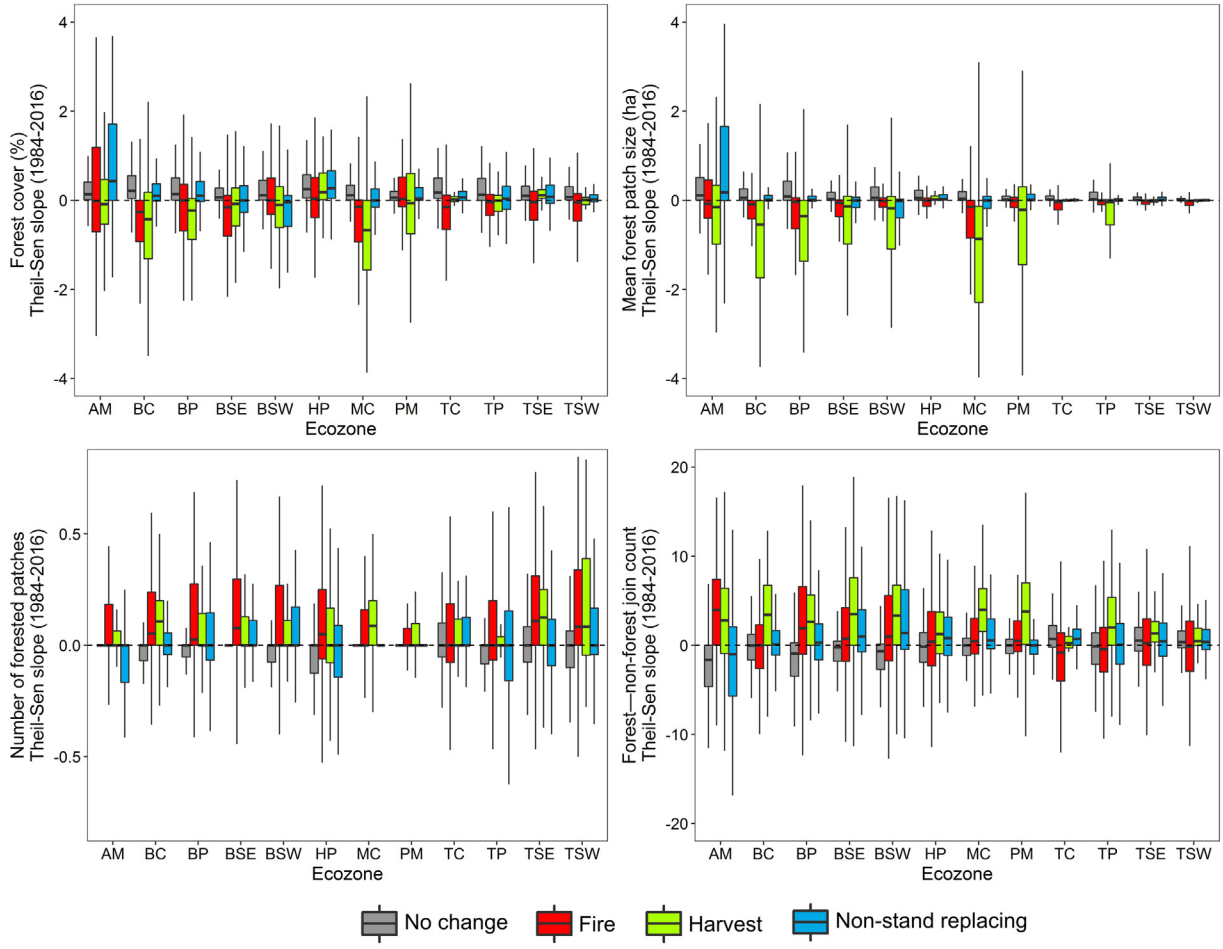

Fig. 7. Distribution of the Theil-Sen slopes of the forest fragmentation metrics (a) forest cover, (b) mean forest patch size, (c) number of forested patches, and (d) forest–non-forest join count, by forested ecozone. (AM: Atlantic Maritime; BC: Boreal Cordillera; BP: Boreal Plains; BSE: Boreal Shield East; BSW: Boreal Shield West; HP: Hudson Plains; MC: Montane Cordillera; PM: Pacific Maritime; TC: Taiga Cordillera; TP: Taiga Plains TSE: Taiga Shield East; TSW: Taiga Shield West). Boxplots represent median, interquartile range, and extreme values. Note that outliers are not displayed.

values of fragmentation metrics in these unchanged areas indicated a successive reduction in fragmentation as forests develop, indicative of the natural growth and expansion of the treed vegetation (Fig. 5). These trends convey the regional dynamics of various stand development stages, as they represent mature forest, but also young forests recovering from disturbances that occurred prior to 1984 (i.e., before the analysis period; Matasci et al., 2018).

The multi-temporal assessment presented herein affirms results for a single-date assessment of forest fragmentation in Canada for circa 2000 (Wulder et al., 2011, 2008a). In this assessment, the Taiga Shield and Taiga Cordillera were likewise identified as having more fragmented forests circa 2000, and these were also the ecozones that had the lowest proportion of forest cover (Wulder et al., 2008a). These ecozones were considered to be inherently fragmented as a result of prolific water features (Taiga Shield) and extreme topography (Taiga Cordillera; Wulder et al., 2011). Conversely, the Atlantic Maritime was identified as one of the least fragmented ecozones; however, as roads are the primary driver of fragmentation in this ecozone, the level of fragmentation in this ecozone is likely underestimated (Wulder et al., 2011), since Landsat is not an optimal tool for road detection and mapping. Previous research has demonstrated that harvesting results in more fragmented landscapes than natural disturbances (Hudak et al., 2007; Tinker et al., 1998). We likewise found that harvesting activities lead to an increase of fragmentation, with negative median Theil-Shen slopes for forest cover and mean forest patch size. Fires resulted in an increased fragmentation in the configuration of forests, with the highest positive median Theil-Shen slopes for number of forested patches. In part, these trends may be explained by the fact that harvesting typically occurs in highly productive areas with greater pre-disturbance forest cover (Fig. 9) and less fragmentation. In contrast fires typically occur in a more diverse range of forest conditions and land cover types, and tend to be more patchy and of variable intensity (White et al., 2017). The results presented herein indicate that forest fragmentation dynamics after fire and harvesting differ. While harvesting resulted in more fragmented landscapes than fire immediately following disturbance events, fragmentation metrics returned to pre-disturbance values more rapidly following harvest compared to fire. Areas impacted by fires had lower pre-disturbance forest cover (Fig. 9), and were characterized by an increasing forest–non-forest join count (Fig. 8). The evolution of forest fragmentation patterns in harvest-dominated landscapes is also influenced by mandated replanting activities (following jurisdictional sustainable forest management regulations) and more productive sites that lead to more rapidly reaching a forest fragmentation baseline. The impacts of non-stand replacing changes on landscapes can be notable related to the health and status of vegetation (e.g., insect infestations or drought stress), however they do not involve a major short- or long-term alteration of the forest fragmentation patterns captured. For example, insect-related disturbances generally result in widespread tree damage and mortality (Senf et al., 2015), but not in a broad-scale (immediate) removal of treed vegetation (Hall et al., 2016).

Mapping and consideration of forest fragmentation through time enables national monitoring of fragmentation dynamics (i.e., increases

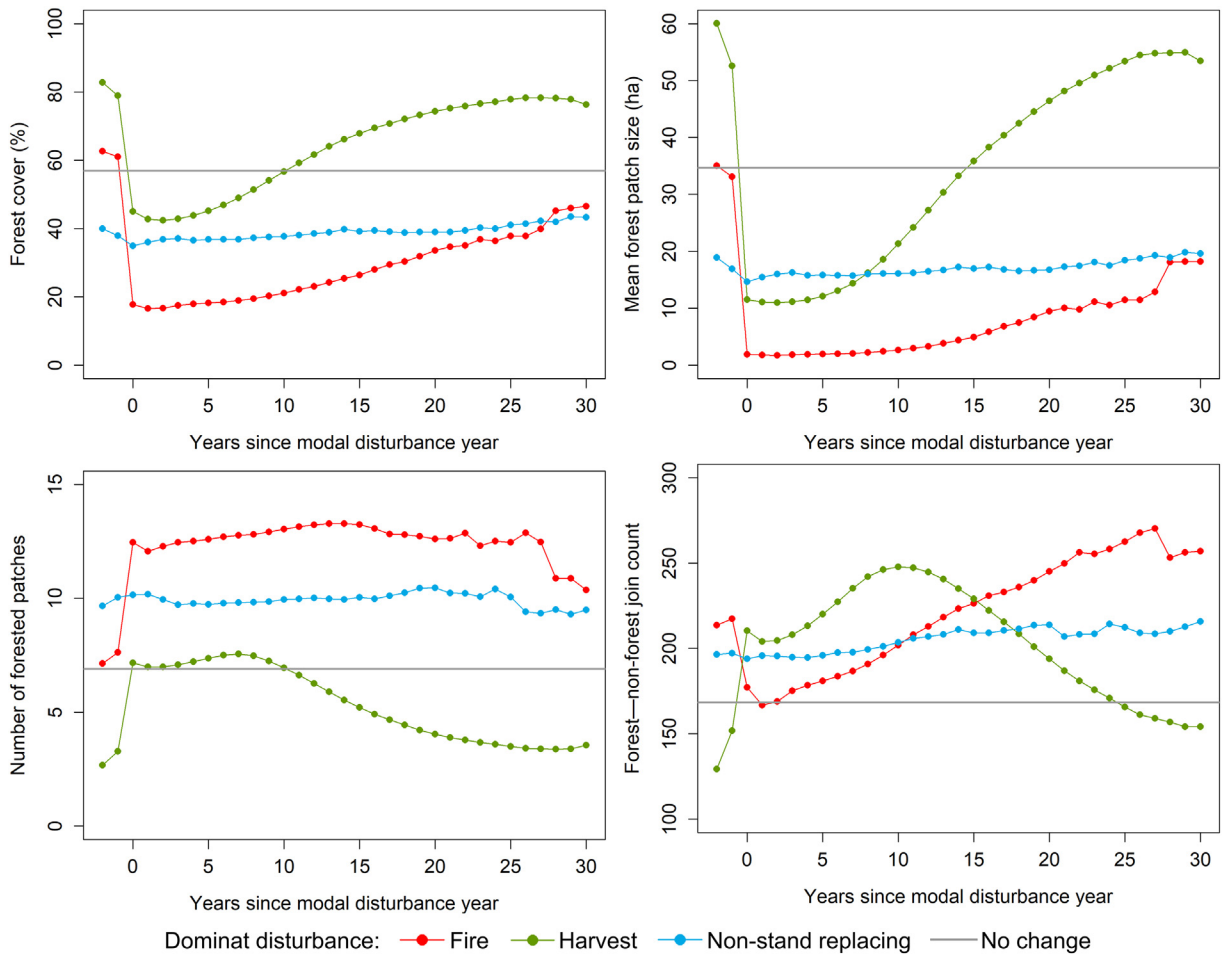

Fig. 8. Mean values of the forest fragmentation metrics for the disturbance-dominated landscapes across Canada's forested ecosystems. X-axis shows years since the modal disturbance year for the dominant disturbance type.

or decreases in measures of pattern and distribution of treed vegetation; Fig. 2), but also enable the analysis of trends in forest fragmentation patterns by disturbance types. Fig. 3 highlights highly dynamic areas with various marked positive and negative forest fragmentation trends in the studied metrics. Fig. 3a displays the effect on forest fragmentation produced by increased harvest activity in the mid-2000's in response to infestation by mountain pine beetle (*Dendroctonus ponderosae*) in the Montane Cordillera (Wulder et al., 2009), which led to an overall decrease of forest cover and an increase of forest–non-forest interface. Areas dominated by wildfire, such as northern Saskatchewan (Fig. 3b), show significant trends of both increasing and decreasing fragmentation. The sign and magnitude of these temporal trends is mainly impacted by when the event occurred within the analysis period. Fires occurring early in the time series resulted in a decrease in forest fragmentation, while fires occurring at the end of the analysis period resulted in an increase in forest fragmentation. The Hudson Plains (Fig. 3c) show significantly increasing trends of forest cover and mean forest patch size, and a marked reduction in the number of forest patches. Hudson Plains is a notably distinct ecozone dominated by wetlands with an increase in treed cover possibly related to transition from wetland to wetland treed areas (Wulder et al., 2018b). Ballantyne and Nol (2015) documented an increase in shrub and tree cover over the period 1973 to 2006 of 12.6 and 6.9%, respectively. Finally, Fig. 3d shows the fragmentation dynamics as response to localized weather events, such as an extensive area located in the Boreal Shield East (Lake Nipigon ecoregion) which was damaged by an early and heavy snow fall event (October 24, 2001; described in Wulder et al., 2010). This specific event caused an increase in forest fragmentation indicated by significant reductions of canopy cover and mean forest patch size, and an increased number of forested patches and more forest–non-forest join counts.

5.2. *Analysis of forest fragmentation using Landsat time-series data: insights and considerations*

Free and open access to the Landsat data archive has facilitated new opportunities for monitoring large-forested areas through time (Wulder et al., 2018a). Motivated by information needs around monitoring forests for inventory and carbon accounting purposes, among others (White et al., 2014), time series of Landsat surface-reflectance composites have enabled generation of Canada-wide annual, temporally-consistent land cover maps. These map products provide the capacity to observe and describe baseline levels of forest fragmentation in areas that have not changed within the analysis period, and also the different patterns and dynamics following stand-replacing and non-stand-replacing disturbances. Historically, the study of forest fragmentation using remotely sensed data has been limited by availability and access to data. This restricted the temporal scale of the analysis to the depiction of forest fragmentation as a state by considering a single date (Cardille et al., 2005; Riitters et al., 2002; Wulder et al., 2011, 2008a) or limited epochal analyses (Çakir et al., 2008; Coops et al., 2010; Margono et al., 2012; Wickham et al., 2008). The use of annual time series provide the ability to further assess the change of the forest fragmentation provided by contrasting two or few more dates, by enabling a more detailed description of fragmentation patterns' trends and evolution (Pickell et al., 2016a). In addition, annual information on forest fragmentation

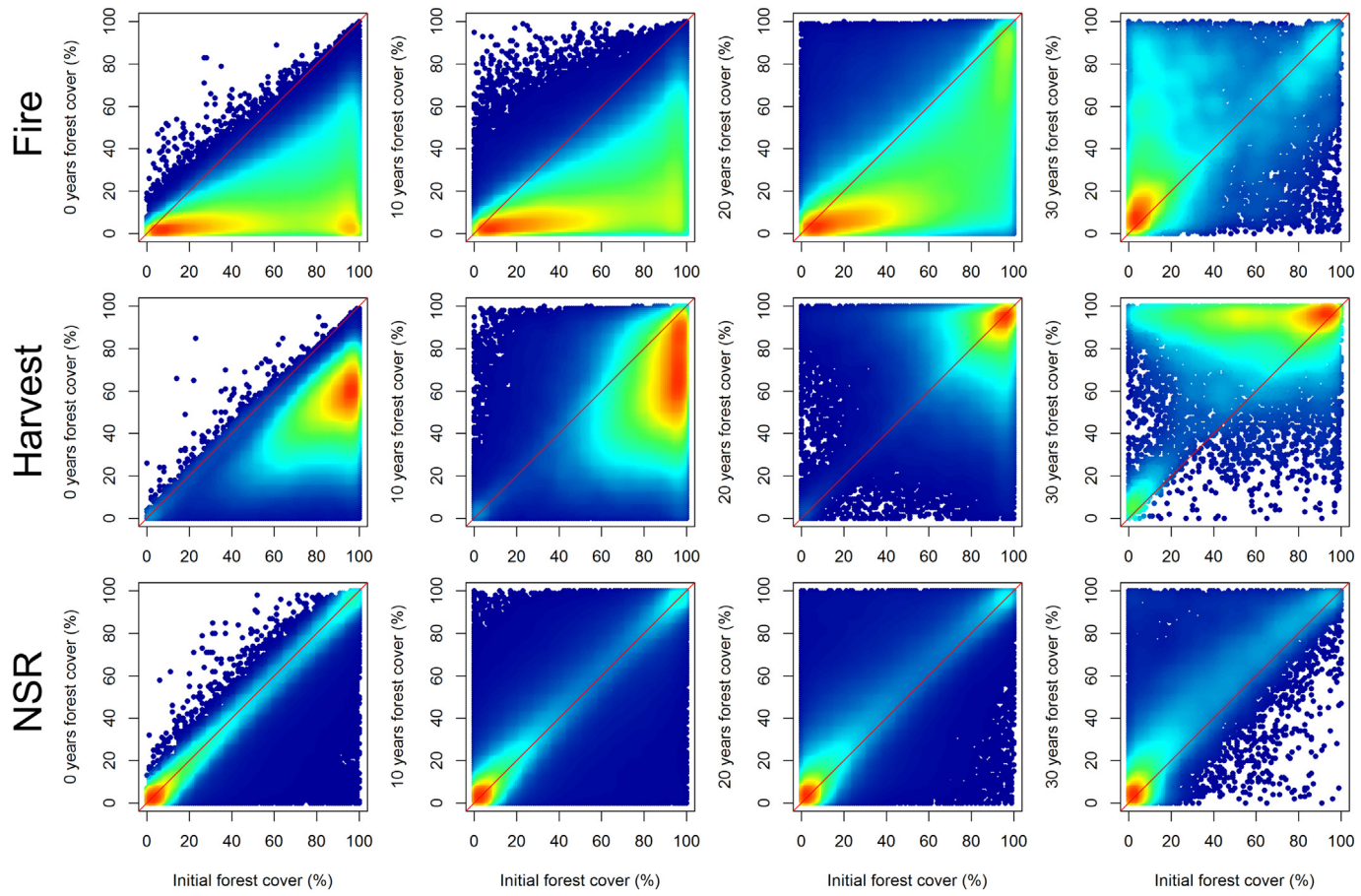

Fig. 9. Chronosequence of heat-map scatterplots showing the relationships between forest cover before and 0, 10, 20, and 30 years following modal disturbance events for fire, harvest, and non-stand replacing (NSR) changes. Note that the sample population across the analyzed period is variable, with a greater number of landscape units within a shorter time since modal disturbance and a lesser number of landscape units with longer periods of time since disturbance. Values above the 1:1 diagonal line indicate higher forest cover after disturbance and values below the 1:1 line indicate lower forest cover after disturbance.

permits a more complete portrayal of the different temporal manifestations of the spatial configuration of forests following disturbance events.

The 33-year time period covered by this study (1984–2016) at an annual time-step provides useful data and information with regards to monitoring forest fragmentation dynamics following change events. Although exceeding three decades, the length of the analysis period may not be sufficiently long to capture the return to the spatial patterns present prior to disturbance, especially in more northern, slow growing, lower productivity, forest environments (Bolton et al., 2017). Moreover, the timing of disturbances relative to the analysis period appears to be of importance for characterizing forest fragmentation dynamics post-disturbance. For example, change events that occurred before or at the beginning of the analysis period will show stronger vegetation recovery trends, with concomitant increases in forest cover, mean patch size, and a reduction in the number of forest patches. On the other hand, disturbances occurring near the end of the analyzed time window will likely be represented by increasing fragmentation trends. Longer analysis periods are expected to moderate these disturbance effects on the fragmentation trends (Pickell et al., 2016a). Alternatively, fragmentation trends might be analyzed considering multiple periods based on time since disturbance events (Tavernia et al., 2016). Moving forward, the ability to consider longer periods will be made possible by the images currently collected by Landsat-8 OLI and Sentinel-2, and by the on-going development and scheduled December 2020 launch of Landsat 9. Furthermore, recent advances in product development are increasing the potential to use Landsat MSS imagery to extend the monitoring analysis backwards until 1972 (Savage et al., 2018), presenting an additional opportunity to extend the temporal analysis window.

The study presented herein was made possible due to the high density of coverage over Canada's forested ecosystems by the Landsat archive (White and Wulder, 2014). However, it might be challenging to obtain enough clear observations in other regions of the world such as tropical latitudes or areas where ground receiving stations were only installed in later years. While initiatives such as the global archive consolidation (Wulder et al., 2016) have significantly increased the Landsat data holdings for some areas globally, the density and temporal distribution of these images might not be optimal to conduct analogous analyses. Thus, imagery with lower spatial resolution (e.g., MODIS) might be required to ensure the spatial coverage, but may otherwise hinder detailed spatial and temporal analyses of forest fragmentation patterns at spatial scales meaningful to forest management and reporting activities. Moreover, the different spatial resolution of the MODIS data may result in different fragmentation metric values (e.g. Nelson et al., 2009). While data blending opportunities to bring together Landsat and MODIS data do exist (Gao et al., 2006) and could provide data suitable for analysis (Hilker et al., 2009), the baseline would be limited to following the 1999 launch of MODIS. Further, our analyses characterize the temporal trends in the forest fragmentation metrics, given a consistently generated data source (Hermosilla et al., 2018) and a size-invariant analysis unit (1 × 1 km). Although previous research has shown that fragmentation metrics are impacted by the size of the landscape analysis unit chosen, ecozonal trends in metric values are relatively stable across different spatial scales, with absolute (count-based) metrics impacted by analysis unit size more than metrics standardized to the area of the landscape analysis unit (Gergel, 2006;

Wulder et al., 2008a). Consequently, temporal trends resulting from forest fragmentation analyses at different spatial scales are expected to be consistent; however, the significance of these temporal trends may differ (Pickell et al., 2016a).

This research provides additional understanding of the forest dynamics present over Canada's forested ecosystems. Uniquely, this analysis of time series of Landsat data has enabled insight on the dynamics of spatial patterns and how this relates to the reestablishment of treed vegetation following disturbance. As described above, given sufficient time following disturbance, the pre-disturbance spatial patterns are shown to return. These results complement forest recovery findings based upon spectral (Frazier et al., 2018; Pickell et al., 2016b; White et al., 2017) and land cover (Hermosilla et al., 2018) interpretations. Furthermore, in Matasci et al. (2018) using forest structural attributes (e.g., height, biomass, cover), generated from a 33-yeartime series of Landsat and samples of lidar data the reestablishment of treed vegetation following disturbance is shown. The results presented here complement the spectral, land cover, and vertical structural analyses of forest dynamics, and show the ability of spatially describing the return of treed-vegetation patterns, complementing our understanding of forest recovery from a number of perspectives as produced by different disturbance events.

6. Conclusions

Using an annual series of land cover maps produced from Landsat imagery enables an augmented and detailed assessment of forest fragmentation and fragmentation dynamics in forested ecosystems. Herein, we established a baseline of forest fragmentation nationally and for each ecozone through the characterization of the existing fragmentation in unchanged areas of Canada's forested ecozones. By examining annual values of fragmentation metrics, we characterized temporal trends in the evolution of forest fragmentation in environments dominated by disturbances (i.e., fire, harvest, non-stand replacing changes) and in areas that did not experience disturbances during the analysis period (1984–2016). The analysis of forest fragmentation following disturbance events enabled us to monitor the recovery of spatial patterns as treed-vegetation re-established, complementing spectral and vertical structural measures of forest recovery. Transferring the methods presented herein to other study areas may require modification in order to address regional particularities of forest management practices, disturbance regimes, and recovery rates. Nevertheless, the logic and methods presented in this study offer an approach that can be adapted to different forested ecosystems globally to enhance our understanding of forest fragmentation dynamics and the recovery of spatial patterns after disturbance events.

Acknowledgments

This research was undertaken as part of the “Earth Observation to Inform Canada's Climate Change Agenda (EO3C)” project jointly funded by the Canadian Space Agency's (CSA) Government Related Initiatives Program (GRIP), and the Canadian Forest Service (CFS) of Natural Resources Canada (NRCan). Geordie Hobart, of the Canadian Forest Service, is thanked for his assistance in acquiring the Landsat data and preparing the annual best-available pixel image composites. This research was enabled in part by support provided by WestGrid (www.westgrid.ca) and Compute Canada (www.computecanada.ca).

References

Abercrombie, S.P., Friedl, M.A., 2016. Improving the consistency of multitemporal land cover maps using a hidden Markov model. IEEE Trans. Geosci. Remote Sens. 54, 703–713. https://doi.org/10.1109/TGRS.2015.2463689.

Ballantyne, K., Nol, E., 2015. Localized habitat change near Churchill, Manitoba and the decline of nesting whimbrels (*Numenius phaeopus*). Polar Biol. 38, 529–537. https://doi.org/10.1007/s00300-014-1615-6.

Betts, M.G., 2000. In Search of Ecological Relevancy: A Review of Landscape Fragmentation Metrics and Their Application for the Fundy Model. University of New Brunswick, Fredericton, NB.

Boentje, J.P., Blinnikov, M.S., 2007. Post-Soviet forest fragmentation and loss in the Green Belt around Moscow, Russia (1991–2001): a remote sensing perspective. Landsc. Urban Plan. 82, 208–221. https://doi.org/10.1016/j.landurbplan.2007.02.009.

Bolton, D.K., Coops, N.C., Hermosilla, T., Wulder, M.A., White, J.C., 2017. Assessing variability in post-fire forest structure along gradients of productivity in the Canadian boreal using multi-source remote sensing. J. Biogeogr. 44, 1294–1305. https://doi.org/10.1111/jbi.12947.

Boots, B., 2005. Local configuration measures for categorical spatial data: binary regular lattices. J. Geogr. Syst. 8, 1–24. https://doi.org/10.1007/s10109-005-0010-9.

Butler, B.J., Swenson, J.J., Alig, R.J., 2004. Forest fragmentation in the Pacific northwest: quantification and correlations. For. Ecol. Manag. 189, 363–373. https://doi.org/10.1016/j.foreco.2003.09.013.

Çakir, G., Sivrikaya, F., Keleş, S., 2008. Forest cover change and fragmentation using Landsat data in Maçka State Forest Enterprise in Turkey. Environ. Monit. Assess. 137, 51–66. https://doi.org/10.1007/s10661-007-9728-9.

Cardille, J.A., Turner, M., Clayton, M.K., Gergel, S., Price, S., 2005. METALAND: characterizing spatial patterns and statistical context of landscape metrics. Bioscience 55, 983–988. https://doi.org/10.1641/0006-3568(2005)055.

Cohen, W.B., Goward, S.N., 2004. Landsat's role in ecological applications of remote sensing. Bioscience 54, 535. https://doi.org/10.1641/0006-3568(2004)054[0535:LRIEAO]2.0.CO;2.

Coops, N.C., Gillanders, S.N., Wulder, M.A., Gergel, S.E., Nelson, T.A., Goodwin, N.R., 2010. Assessing changes in forest fragmentation following infestation using time series Landsat imagery. For. Ecol. Manag. 259, 2355–2365. https://doi.org/10.1016/j.foreco.2010.03.008.

Ecological Stratification Working Group, 1995. A National Ecological Framework for Canada. 0-662-24107-X (https://doi.org/Cat., No. A42-65/1996E).

Fahrig, L., 2003. Effects of habitat fragmentation on biodiversity. Annu. Rev. Ecol. Evol. Syst. 34, 487–515. https://doi.org/10.1146/annurev.ecolsys.34.011802.132419.

Frazier, R.J., Coops, N.C., Wulder, M.A., 2015. Boreal shield forest disturbance and recovery trends using Landsat time series. Remote Sens. Environ. 170, 317–327. https://doi.org/10.1016/j.rse.2015.09.015.

Frazier, R.J., Coops, N.C., Wulder, M.A., Hermosilla, T., White, J.C., 2018. Analyzing spatial and temporal variability in short-term rates of post-fire vegetation return from Landsat time series. Remote Sens. Environ. 205, 32–45. https://doi.org/10.1016/j.rse.2017.11.007.

Gao, F., Masek, J.G., Schwaller, M., Hall, F., 2006. On the blending of the Landsat and MODIS surface reflectance: predicting daily Landsat surface reflectance. IEEE Trans. Geosci. Remote Sens. 44, 2207–2218. https://doi.org/10.1109/TGRS.2006.872081.

Gergel, S.E., 2006. New directions in landscape pattern analysis and linkages with remote sensing. In: Wulder, M.A., Franklin, S.E. (Eds.), Understanding Forest Disturbance and Spatial Pattern: Remote Sensing and GIS Approaches. Taylor and Francis, Boca Raton, FL, USA, pp. 173–208.

Gómez, C., White, J.C., Wulder, M.A., 2016. Optical remotely sensed time series data for land cover classification: a review. ISPRS J. Photogramm. Remote Sens. 116, 55–72. https://doi.org/10.1016/j.isprsjprs.2016.03.008.

Gustafson, E., 1998. Pattern: what is the state of the art? Ecosystems 143–156. https://doi.org/10.1007/s100219900011.

Hall, R.J., Castilla, G., White, J.C., Cooke, B.J., Skakun, R.S., 2016. Remote sensing of forest pest damage: a review and lessons learned from a Canadian perspective. Can. Entomol. 148, S296–S356. https://doi.org/10.4039/tce.2016.11.

Hansen, M.C., Potapov, P.V., Moore, R., Hancher, M., Turubanova, S.A., Tyukavina, A., Thau, D., Stehman, S.V., Goetz, S.J., Loveland, T.R., Kommareddy, A., Egorov, A., Chini, L., Justice, C.O., Townshend, J.R.G., 2013. High-resolution global maps of 21st-century forest cover change. Science 342, 850–853. https://doi.org/10.1126/science.1244693.

Hermosilla, T., Wulder, M.A., White, J.C., Coops, N.C., Hobart, G.W., 2015a. An integrated Landsat time series protocol for change detection and generation of annual gap-free surface reflectance composites. Remote Sens. Environ. 158, 220–234. https://doi.org/10.1016/j.rse.2014.11.005.

Hermosilla, T., Wulder, M.A., White, J.C., Coops, N.C., Hobart, G.W., 2015b. Regional detection, characterization, and attribution of annual forest change from 1984 to 2012 using Landsat-derived time-series metrics. Remote Sens. Environ. 170, 121–132. https://doi.org/10.1016/j.rse.2015.09.004.

Hermosilla, T., Wulder, M.A., White, J.C., Coops, N.C., Hobart, G.W., Campbell, L.B., 2016. Mass data processing of time series Landsat imagery: pixels to data products for forest monitoring. Int. J. Digital Earth 9, 1035–1054. https://doi.org/10.1080/17538947.2016.1187673.

Hermosilla, T., Wulder, M.A., White, J.C., Coops, N.C., Hobart, G.W., 2017. Updating Landsat time series of surface-reflectance composites and forest change products with new observations. Int. J. Appl. Earth Obs. Geoinf. 63, 104–111. https://doi.org/10.1016/j.jag.2017.07.013.

Hermosilla, T., Wulder, M.A., White, J.C., Coops, N.C., Hobart, G.W., 2018. Disturbance-informed annual land cover classification maps of Canada's forested ecosystems for a 29-year Landsat time series. Can. J. Remote. Sens. 44, 67–87. https://doi.org/10.1080/07038992.2018.1437719.

Hilker, T., Wulder, M.A., Coops, N.C., Seitz, N., White, J.C., Gao, F., Masek, J.G., Stenhouse, G., Linke, J., McDermid, G., 2009. Generation of dense time series synthetic Landsat data through data blending with MODIS using a spatial and temporal adaptive reflectance fusion model. Remote Sens. Environ. 113, 1988–1999. https://doi.org/10.1016/j.rse.2009.05.011.

Hudak, A.T., Morgan, P., Bobbitt, M., Lentile, L., 2007. Characterizing Stand-Replacing

Harvest and Fire Disturbance Patches in a Forested Landscape: A Case Study From Cooney Ridge, Montana. pp. 209–231.
Kendall, M., Gibbons, J.D., 1990. Rank Correlation Methods.
Keogh, E., Chu, S., Hart, D., Pazzani, M., 2001. An online algorithm for segmenting time series. In: Data Mining, 2001. ICDM, Proceedings IEEE International Conference On. IEEE Comput. Soc, San Jose, CA, pp. 289–296. https://doi.org/10.1109/ICDM.2001.989531.
Key, C.H., Benson, N.C., 2006. Landscape Assessment: Sampling and Analysis Methods. USDA for. Serv. Gen. Tech. Rep. RMRS-GTR-164-CD. pp. 1–55.
Li, X., He, H.S., Bu, R., Wen, Q., Chang, Y., Hu, Y., Li, Y., 2005. The adequacy of different landscape metrics for various landscape patterns. Pattern Recogn. 38, 2626–2638. https://doi.org/10.1016/j.patcog.2005.05.009.
Li, M., Huang, C., Zhu, Z., Shi, H., Lu, H., Peng, S., 2009. Assessing rates of forest change and fragmentation in Alabama, USA, using the vegetation change tracker model. For. Ecol. Manag. 257, 1480–1488. https://doi.org/10.1016/j.foreco.2008.12.023.
Long, J.A., Nelson, T.A., Wulder, M.A., 2010. Characterizing forest fragmentation: distinguishing change in composition from configuration. Appl. Geogr. 30, 426–435. https://doi.org/10.1016/j.apgeog.2009.12.002.
Margono, B.A., Turubanova, S., Zhuravleva, I., Potapov, P., Tyukavina, A., Baccini, A., Goetz, S., Hansen, M.C., 2012. Mapping and monitoring deforestation and forest degradation in Sumatra (Indonesia) using Landsat time series data sets from 1990 to 2010. Environ. Res. Lett. 7. https://doi.org/10.1088/1748-9326/7/3/034010.
Masek, J.G., Vermote, E.F., Saleous, N.E., Wolfe, R., Hall, F.G., Huemmrich, K.F., Gao, F., Kutler, J., Lim, T.K., 2006. A Landsat surface reflectance dataset for North America, 1990–2000. IEEE Geosci. Remote Sens. Lett. 3, 68–72.
Matasci, G., Hermosilla, T., Wulder, M.A., White, J.C., Coops, N.C., Hobart, G.W., Bolton, D.K., Tompalski, P., Bater, C.W., 2018. Three decades of forest structural dynamics over Canada's forested ecosystems using Landsat time-series and lidar plots. Remote Sens. Environ. 216, 697–714. https://doi.org/10.1016/j.rse.2018.07.024.
McGarigal, K., Marks, B., 1995. Spatial Pattern Analysis Program for Quantifying Landscape Structure. Gen. Tech. Rep. PNW-GTR-351. US … 97331.
Natural Resources Canada, 2016. The State of Canada's Forests. Annual Report 2016. Ottawa.
Nelson, M.D., McRoberts, R.E., Holden, G.R., Bauer, M.E., 2009. Effects of satellite image spatial aggregation and resolution on estimates of forest land area. Int. J. Remote Sens. 30, 1913–1940. https://doi.org/10.1080/01431160802545631.
Pekel, J.-F., Cottam, A., Gorelick, N., Belward, A.S., 2016. High-resolution mapping of global surface water and its long-term changes. Nature 540, 1–19. https://doi.org/10.1038/nature20584.
Pickell, P.D., Coops, N.C., Gergel, S.E., Andison, D.W., Marshall, P.L., 2016a. Evolution of Canada's boreal forest spatial patterns as seen from space. PLoS One 11, 1–20. https://doi.org/10.1371/journal.pone.0157736.
Pickell, P.D., Hermosilla, T., Frazier, R.J., Coops, N.C., Wulder, M.A., 2016b. Forest recovery trends derived from Landsat time series for north American boreal forests. Int. J. Remote Sens. 37, 138–149. https://doi.org/10.1080/2150704X.2015.1126375.
Rickbeil, G.J.M., Hermosilla, T., Coops, N.C., White, J.C., Wulder, M.A., Lantz, T.C., 2018. Changing northern vegetation conditions are influencing barren ground caribou (*Rangifer tarandus groenlandicus*) post-calving movement rates. J. Biogeogr. 45, 702–712. https://doi.org/10.1111/jbi.13161.
Riitters, K., Wickham, J., Neill, R.O., Jones, B., 2000. Global-scale patterns of forest fragmentation. Conserv. Ecol. 4, 3.
Riitters, K.H., Wickham, J.D., Neill, R.V.O., Jones, K.B., Smith, R., Coulston, J.W., Wade, T.G., Smith, J.H., Smith, E.R., 2002. Fragmentation of Continental United Forests. 5. pp. 815–822. https://doi.org/10.1007/s10021002-0209-2.
Roy, D.P., Ju, J., Kline, K., Scaramuzza, P.L., Kovalskyy, V., Hansen, M., Loveland, T.R., Vermote, E., Zhang, C., 2010. Web-enabled Landsat data (WELD): Landsat ETM+ composited mosaics of the conterminous United States. Remote Sens. Environ. 114, 35–49. https://doi.org/10.1016/j.rse.2009.08.011.
Sanchez-Azofeifa, G.A., Harriss, R.C., Skole, D.L., 2001. Deforestation in Costa Rica: a quantitative analysis using remote sensing imagery. Biotropica 33, 378–384. https://doi.org/10.1111/j.1744-7429.2001.tb00192.x.
Saunders, D.A., Hobbs, R.J., Margules, C.R., 1991. Biological consequences of ecosystem fragmentation: a review. Conserv. Biol. 5, 18–32. https://doi.org/10.1111/j.1523-1739.1991.tb00384.x.
Savage, S.L., Lawrence, R.L., Squires, J.R., Holbrook, J.D., Olson, L.E., Braaten, J.D., Cohen, W.B., 2018. Shifts in forest structure in northwest Montana from 1972 to 2015 using the landsat archive from multispectral scanner to operational land imager. Forests 9, 1–20. https://doi.org/10.3390/f9040157.
Schmidt, G.L., Jenkerson, C.B., Masek, J., Vermote, E., Gao, F., 2013. Landsat Ecosystem Disturbance Adaptive Processing System (LEDAPS) Algorithm Description.
Sen, P.K., 1968. Estimates of the regression coefficient based on Kendall's Tau. J. Am. Stat. Assoc. 63, 1379–1389. https://doi.org/10.1080/01621459.1968.10480934.
Senf, C., Pflugmacher, D., Wulder, M.A., Hostert, P., 2015. Characterizing spectral–temporal patterns of defoliator and bark beetle disturbances using Landsat time series. Remote Sens. Environ. 170, 166–177. https://doi.org/10.1016/j.rse.2015.09.019.
Soverel, N., Coops, N.C., White, J.C., Wulder, M.A., 2010. Characterizing the forest fragmentation of Canada's national parks. Environ. Monit. Assess. 164, 481–499.
Stocks, B.J., Mason, J.A., Todd, J.B., Bosch, E.M., Wotton, B.M., Amiro, B.D., Flannigan, M.D., Hirsch, K.G., Logan, K.A., Martell, D.L., Skinner, W.R., 2002. Large forest fires in Canada, 1959–1997. J. Geophys. Res. 108. https://doi.org/10.1029/2001JD000484.
Tavernia, B.G., Nelson, M.D., Garner, J.D., Perry, C.H., 2016. Spatial characteristics of early successional habitat across the upper Great Lakes states. For. Ecol. Manag. 372, 164–174. https://doi.org/10.1016/j.foreco.2016.04.003.
Tinker, D.B., Resor, C.A.C., Beauvais, G.P., Kipfmueller, K.F., Fernandes, C.I., Baker, W.L., 1998. Watershed analysis of forest fragmentation by clearcuts and roads in a Wyoming forest. Landsc. Ecol. 13, 149–165. https://doi.org/10.1023/A:1007919023983.
Turner, M.G., 1989. Landscape ecology: the effect of pattern on process. Annu. Rev. Ecol. Syst. 20, 171–197.
Turner, M.G., Neill, R.V.O., Gardner, R.H., Milne, B.T., 1989. Effects of changing spatial scale on the analysis of landscape pattern. Landsc. Ecol. 3, 153–162.
Turner, M.G., Donato, D.C., Romme, W.H., 2013. Consequences of spatial heterogeneity for ecosystem services in changing forest landscapes: priorities for future research. Landsc. Ecol. 28, 1081–1097. https://doi.org/10.1007/s10980-012-9741-4.
Vogelmann, J.E., 1995. Assessment of Forest fragmentation in southern New England using remote sensing and geographic information systems technology. Conserv. Biol. 9, 439–449.
White, J.C., Wulder, M.A., 2014. The Landsat observation record of Canada: 1972–2012. Can. J. Remote. Sens. 39, 455–467.
White, J.C., Wulder, M.A., Hobart, G.W., Luther, J.E., Hermosilla, T., Griffiths, P., Coops, N.C., Hall, R.J., Hostert, P., Dyk, A., Guindon, L., 2014. Pixel-based image compositing for large-area dense time series applications and science. Can. J. Remote. Sens. 40, 192–212. https://doi.org/10.1080/07038992.2014.945827.
White, J.C., Wulder, M.A., Hermosilla, T., Coops, N.C., Hobart, G.W., 2017. A nationwide annual characterization of 25 years of forest disturbance and recovery for Canada using Landsat time series. Remote Sens. Environ. 194, 303–321. https://doi.org/10.1016/j.rse.2017.03.035.
Wickham, J.D., Riitters, K.H., Wade, T.G., Homer, C., 2008. Temporal change in fragmentation of continental US forests. Landsc. Ecol. 23, 891–898. https://doi.org/10.1007/s10980-008-9258-z.
Woodcock, C.E., Allen, R., Anderson, M., Belward, A., Bindschadler, R., Cohen, W., Gao, F., Goward, S.N., Helder, D.L., Helmer, E.H., Nemani, R.R., Oreopoulos, L., Schott, J., Thenkabail, P.S., Vermonte, E., Vogelmann, J.E., Wulder, M.A., Wynne, R.H., 2008. Free access to Landsat imagery. Science 80 (320), 1011. https://doi.org/10.1126/science.320.5879.1011a.
Wulder, M.A., White, J., Han, T., Coops, N., Cardille, J.A., Holland, T., Grills, D., 2008a. Monitoring Canada's forests. Part 2: national forest fragmentation and pattern. Can. J. Remote. Sens. 34, 563–584.
Wulder, M.A., White, J.C., Cranny, M.M., Hall, R.J., Luther, J.E., Beaudoin, A., Goodenough, D.G., Dechka, J.A., 2008b. Monitoring Canada's forests. Part 1: completion of the EOSD land cover project. Can. J. Remote. Sens. 34, 549–562.
Wulder, M.A., White, J.C., Goward, S.N., Masek, J.G., Irons, J.R., Herold, M., Cohen, W.B., Loveland, T.R., Woodcock, C.E., 2008c. Landsat continuity: issues and opportunities for land cover monitoring. Remote Sens. Environ. 112, 955–969. https://doi.org/10.1016/j.rse.2007.07.004.
Wulder, M.A., White, J.C., Grills, D., Nelson, T., Coops, N.C., 2009. Aerial overview survey of the mountain pine beetle epidemic in British Columbia: communication of impacts. Br. Columbia J. Ecosyst. Manage. 10, 45–58.
Wulder, M.A., White, J.C., Gillis, M.D., Walsworth, N., Hansen, M.C., Potapov, P., 2010. Multiscale satellite and spatial information and analysis framework in support of a large-area forest monitoring and inventory update. Environ. Monit. Assess. 170, 417–433. https://doi.org/10.1007/s10661-009-1243-8.
Wulder, M.A., White, J.C., Coops, N.C., 2011. Fragmentation regimes of Canada's forests. Can. Geogr. 55, 288–300. https://doi.org/10.1111/j.1541-0064.2010.00335.x.
Wulder, M.A., Masek, J.G., Cohen, W.B., Loveland, T.R., Woodcock, C.E., 2012. Opening the archive: how free data has enabled the science and monitoring promise of Landsat. Remote Sens. Environ. 122, 2–10. https://doi.org/10.1016/j.rse.2012.01.010.
Wulder, M.A., White, J.C., Loveland, T.R., Woodcock, C.E., Belward, A.S., Cohen, W.B., Fosnight, E.A., Shaw, J., Masek, J.G., Roy, D.P., 2016. The global Landsat archive: status, consolidation, and direction. Remote Sens. Environ. 185, 271–283. https://doi.org/10.1016/j.rse.2015.11.032.
Wulder, M.A., Coops, N.C., Roy, D.P., White, J.C., Hermosilla, T., 2018a. Land cover 2.0. Int. J. Remote Sens. 39, 4254–4284. https://doi.org/10.1080/01431161.2018.1452075.
Wulder, M.A., Li, Z., Campbell, E.M., White, J.C., Hobart, G., Hermosilla, T., Coops, N.C., 2018b. A national assessment of wetland status and trends for Canada's forested ecosystems using 33 years of Earth observation satellite data. Remote Sens. 10, 1623.
Zheng, D., Wallin, D.O., Hao, Z., 1997. Rates and patterns of landscape change between 1972 and 1998 in the Changbai Mountain area of China and North Korea. Landsc. Ecol. 12, 241–254.
Zhu, Z., Woodcock, C.E., 2012. Object-based cloud and cloud shadow detection in Landsat imagery. Remote Sens. Environ. 118, 83–94. https://doi.org/10.1016/j.rse.2011.10.028.